Identification the Synergistic Effect of Immune-Related lncRNA KIAA0125 and Vitamin D Metabolism Related Gene CYP24A1 in Periodontitis

Yang Li
Department of Stomatology, Zhongshan Hospital, Fudan University
Ruixue Li
Department of Stomatology, Zhongshan Hospital, Fudan University
Ying Wu
Department of Stomatology, Zhongshan Hospital, Fudan University
Chan-Juan Gong
Department of Stomatology, Zhongshan Hospital, Fudan University
XiaoJun Ding (dingxiaojun051214@163.com)
Department of Stomatology, Zhongshan Hospital, Fudan University

Research Article

Keywords: competing endogenous RNAs (ceRNA), periodontitis, immune infiltration, KIAA0125, CYP24A1

Posted Date: December 11th, 2020

DOI: https://doi.org/10.21203/rs.3.rs-122734/v1

Abstract

Background: Periodontitis is a chronic infectious disease characterized by gingival inflammation and progressive destruction of alveolar bone. The interaction of periodontal plaque microorganisms and host immune response affects the process and progression of periodontitis. However, the specific mechanisms and biomarkers involved in periodontitis remain to be further studied.

Methods: In the present research, we explored the expression profile data of differentially expressed lncRNAs and immune-related mRNAs and constructed the competing endogenous RNAs (ceRNA) network. The CIBERSORT analysis was used to infer the composition of 22 immune cells in periodontitis. The genes in ceRNA network were further screened by weighted gene co-expression network analysis (WGCNA), transcriptomic sequencing and PCR.

Results: Our results indicated that a total of 1 lncRNA (KIAA0125), 3 miRNAs (miR-449c-5p, miR-125a-5p and miR-125b-5p) and 2 mRNAs (CYP24A1, BTG2) were involved in establishing the ceRNA network for periodontitis. The expression of KIAA0125 was highly correlated with plasma cells and B cells markers. The WGCNA and transcriptomic sequencing screened out the key gene as the vitamin D metabolic enzyme CYP24A1. The experimental results showed both KIAA0125 and CYP24A1 were highly expressed in the periodontitis gingival tissues. In vitro experiments, the expression of KIAA0125 in human periodontal ligament cells (hPDLCs) were increased after the treatment of lipopolysaccharide and 1,25-dihydroxyvitamin D3 (1,25D) ($P < 0.05$). In addition, we found that 1,25D could alleviate the inflammation of LPS-induced hPDLCs, while the increased expression of KIAA0125 and CYP24A1 would antagonize the anti-inflammatory effect.

Conclusion: In conclusion, immune-related lncRNA KIAA0125 and vitamin D metabolism related gene CYP24A1 can be used as potential diagnostic indicators of periodontitis.

Background

Periodontitis is a chronic infectious disease with plaque biofilm as the main pathogenic factor. Its main clinical manifestations include gingival inflammation and bleeding, alveolar bone resorption, loss of attachment and formation of periodontal pockets, which can eventually lead to tooth loss and seriously affect the quality of life of patients [1]. Periodontal inflammation is the result of the interaction between host immune defense mechanism and microorganisms in dental plaque biofilm. Although bacteria play an indispensable role in the initiation of periodontal inflammation, the progression and severity of the disease depend on the host's immune response [2].

Long non-coding RNA (lncRNA) is a transcription of non-coding proteins with a length of more than 200 nucleotides, which plays a regulatory function directly in the form of RNA [3]. At present, some studies have shown that lncRNA has a variety of biological regulatory functions, including histone modification, chromatin remodeling and genomic imprinting, transcription, splicing, translation, degradation, and transport. LncRNA can be involved in the regulation of gene expression at epigenetic, transcriptional and

post-transcriptional levels, thus affecting the occurrence and development of diseases [4-5]. Currently, some studies have shown that lncRNA is closely related to the occurrence and development of pulpitis, periodontitis and maxillofacial tumors [6-8].

In this study, we explored the phenomenon of immune cell infiltration involved in the pathogenesis of periodontitis, so as to further discover the immune related lncRNAs in periodontitis. In addition, we also constructed the competing endogenous RNAs (ceRNA) network and screened out the key genes by weighted gene co-expression network analysis (WGCNA), transcriptomic sequencing and quantitative real-time PCR (qRT-PCR) results. Through the immune-related lncRNA and key genes in ceRNA network can further comprehensively understand the pathogenesis of periodontitis.

Materials And Methods

Datasets and data processing

We downloaded the gene expression data of 183 cases of periodontitis and 64 cases of normal tissue from the dataset GSE10334 (https://www.ncbi.nlm.nih.gov/geo/query/acc.cgi?acc=GSE10334) from the Gene Expression Omnibus (GEO) and preprocessed the original data using the RMA method. Next, the "Limma" package of R software was used to screen out differentially expressed genes (DEGs) and differentially expressed lncRNAs (DElncRNAs) associated with periodontitis and the screening criteria were |log (FC)| > 1 and adjusted P value < 0.05 [9]. We used the“Pheatmap”package of R software to draw the corresponding heatmap. In order to correlate functional genes with each lncRNAs, co-expression analysis was performed on DElncRNAs and DEGs with the correlation coefficient greater than 0.5 with P value < 0.001. Then, Cytoscape software was used to construct the integrated network [10].

Abundance calculations

CIBERSORT is a tool for deconvolving the expression matrix of immune cell subtypes based on the principle of linear support vector regression. The expression data of RNA-Seq can be used to estimate the infiltration of 22 immune cells, thus quantifying the abundance of specific cell types [11]. Therefore, we used CIBERSORT to calculate differences in immune cell infiltration between normal and periodontitis tissues.

Identification of Immune-Related lncRNAs

The ImmPort database (https://www.immport.org/) contains an updated list of IRGs participating in immunizations [12]. We downloaded all the IRGs from it and used R software to take the intersection of IRGs and DEGs in GSE10334, and then we screened the differentially expressed IRGs. The filtering criterion was |log (FC)| > 1, and the adjusted P value < 0.05. Then Pearson co-expression analysis of differentially expressed lncRNAs and IRGs was performed and the absolute value of Pearson correlation coefficient > 0.6 and P < 0.001. The Cytoscape software was used to construct a visual co-expression network. Subsequently, the relationship between immune cell types and immune-related lncRNAs was then calculated by Pearson analysis.

Explore the ceRNA network

The miRcode database (http://www.mircode.org/) can provide lncRNA-miRNA interaction relationship, so we used this database to predict miRNAs combining with the above immune-related lncRNAs [13]. Then we respectively used miRDB (http://mirdb.org/), TargetScan (http://www.targetscan.org/vert_72/) and miRTarBase database (http://mirtarbase.mbc.nctu.edu.tw/php/index.php) to predict the mRNAs that target with the above miRNAs [14–16]. The resulting target mRNAs were intersected with IRGs. Then Cytoscape software was used to visualize the lncRNA-miRNA-mRNA network. The results showed that only lncRNA KIAA0125 could construct the corresponding ceRNA network, while the remaining three lncRNAs could not predict the targeting effect of miRNAs.

Identification and validation of hub genes by weighted gene co-expression network analysis (WGCNA)

In order to further verify the accuracy of the lncRNAs, miRNAs and mRNAs above, WGCNA analysis method was used for verification. The WGCNA analysis approach aims to find gene modules that are co-expressed and to explore the association between gene networks and phenotypes of concern, as well as the core genes in the networks. Therefore, we downloaded the gene expression of 69 normal tissue and 241 periodontitis from GSE16134 (https://www.ncbi.nlm.nih.gov/geo/query/acc.cgi?acc=GSE16134) and selected the top 25% of genes with the largest variance to construct the weighted gene network by using "WGCNA" package of R software. First we set a threshold β to establish an adjacency matrix based on connectivity so that the distribution of genes conforms to a scale-free network. The adjacency matrix and topology matrix were obtained according to the β value, and the genes were clustered with dissimilarity between genes. We used hierarchical clustering to generate the clustering gene dendrogram and set the minimum module size to 50. The modules with correlation coefficient greater than 0.75 were merged and the corresponding sample dendrogram was drawn. Next, we drew the heatmap of correlation between modules and sample traits, with rows representing modules and columns representing traits. In order to find hub genes related to the trait, we calculated gene significance (GS) and module membership (MM) to observe whether these genes were highly correlated with their corresponding modules and traits [17].

RNA sequence

Total RNA was extracted from 1 gingival tissues with lesions from patients diagnosed with periodontitis and 2 healthy gingival tissues from patients with tooth extraction for orthodontic treatment. The study was approved by Ethical Committee at Zhongshan Hospital. Total RNA was extracted from the tissue using TRIzol® Reagent (Invitrogen) according the manufacturer's instructions and genomic DNA was removed using DNase I (TaKara). RNA-seq transcriptome librariy was prepared following TruSeqTM RNA sample preparation Kit from Illumina (San Diego, CA) using 5 μg of total RNA. Paired-end RNA-seq sequencing library was sequenced with the Illumina HiSeq 4000 (2 × 150 bp read length). To identify DEGs between different samples, the expression level of each transcript was calculated according to the fragments per kilobase of exon per million mapped reads (FRKM) method. RSEM

(http://deweylab.biostat.wisc.edu/rsem/) [18] was used to quantify gene abundances. R statistical package software edgeR [19] was utilized for differential expression analysis. Venn diagram was performed by online tool jvenn (http://bioinformatics.psb.ugent.be/webtools/Venn/) to overlap the DEGs.

Human tissue specimens

In order to verify whether immune-related lncRNA KIAA0125 and CYP24A1 are highly expressed in periodontitis tissue, we obtained diseased gingival tissue of 12 patients with periodontitis (6 females, 6 males) and healthy gingival tissue of 13 patients with tooth extraction orthodontic (6 females, 7 males) and analyzed the expression of related genes. Informed consent was given to all participants. The study was approved by Ethical Committee at Zhongshan Hospital (NO. B2020-128R).

Isolation and cultivation of human periodontal ligament cells (hPDLCs)

Scrape the healthy periodontal ligament tissues at the one-third of the root of premolars that removed during orthodontic treatment. Tissues were transferred to a 6 cm culture dish with DMEM supplemented with 20% fetal bovine serum (CSFBS1050, Cellsera Rutherford, Australia), and cultured at 37 °C in a 5% CO2 humidified atmosphere. hPDLCs crawled out about a week later and were transferred to a 25 m^2 culture flask. Cells at passages 4 to 6 were used for later experiments.

Cell viability assay

Cell activity was measured by a CCK-8 assay (KitkGA317S-500, KeyGEN BioTECH, China). hPDLCs were cultured in 96-well plates and treated with Pg-LPS (InvivoGen, San Diego, USA) at different concentrations (0, 0.1, 1, 5, 10, and 20 μg/ml) for 24 hours. CCK-8 solution was added to each well for 10 μL and incubated at 37℃ for 3 hours for the cell viability assay. Cell viability was determined by reading absorbance at 450 nm using a microplate reader.

Cell stimulation

hPDLCs were seeded in 6-well plates and divided into the following two groups—the control group and Pg-LPS treatment group (LPS) to observe the key genes expressions. Besides, in order to explore whether KIAA0125 and CYP24A1 have a co-expression relationship in an inflammatory environment, hPDLCs were divided into four groups: Pg-LPS treatment group (LPS), 1,25-dihydroxyvitamin D3 (1,25D) (Sigma Aldrich, Saint Louis, MO, USA) and Pg-LPS treatment group (1,25D + LPS), 1,25D and Pg-LPS plus low concentrations of ketoconazole (MedChem Express, Monmouth Junction, USA) group (1,25D + LPS + 10 μM ketoconazole), and 1,25D and Pg-LPS plus high concentrations of ketoconazole group (1,25D + LPS + 100 μM ketoconazole). The concentration of Pg-LPS was 1 μg/mL and 1,25D was 10 nM. The incubation period was 24 hours.

Analysis of gene expression by qRT-PCR

Total RNAs from the above samples were extracted by the TRIzol reagent (T9424-100ML, Sigma Aldrich, Saint Louis, MO, USA) according to the manufacturer's guidance. PrimeScript TMRT Reagent Kit with

gDNA Eraser (RR047A, TaKaRa, Japan) was used to reverse transcribe the extracted RNA into complementary DNA (cDNA) according to the manufacturer's procedure. qRT-PCR was conducted by TB Green Premix Ex Taq (RR420A, TaKaRa, Japan) following the manufacturer protocol through the QuantStudio 5 PCR system (Applied Biosystems, USA). Internal reference was GAPDH. All specific primers were shown as follows: GAPDH forward primer 5'-GAAGGTGAAGGTCGGAGTC-3'; GAPDH reverse primer 5'-GAAGATGGTGATGGGATTTC-3'. KIAA0125 forward primer 5'-CACCATGCGACTTCTTCCCT-3'; KIAA0125 reverse primer 5'-AGTTTCTTCCCTGTGCGGAG-3'; CYP24A1 forward primer 5'-AAAGTATCTGCCTCGTGTTGTA-3'; CYP24A1 reverse primer 5'-CTTCTCTAACCGGTTGTCGATA-3'; CD19 forward primer 5'-AGAGGGAGATAACGCTGTGCTG-3'; CD19 reverse primer 5'-CCCCATCTGTTGAGAGACGTTG-3'; CD79A forward primer 5'-GCAACGAGTCATACCAGCAG-3'; CD79A reverse primer 5'-TCGTTCTGCCATCGTTTCCTG-3'. IL1B forward primer 5'-TTAAAGCCCGCCTGACAGA-3'; IL1B reverse primer 5'-GCGAATGACAGAGGGTTTCTTAG-3'. IL6 forward primer 5'-ACTCACCTCTTCAGAACGAATTG-3'; IL6 reverse primer 5'-CCATCTTTGGAAGGTTCAGGTTG-3'.

Statistical analysis

We analyzed the experimental data and mapped the experimental results using GraphPad Prism 8.0. All results are expressed as the mean ± standard deviation (SD). Comparison between the two groups of samples using Student T test and differences among more than two groups were analyzed by one-way ANOVA test. Results with a $P < 0.05$ were considered statistically significant.

Results

Identification of DEGs and DElncRNAs in periodontitis

After setting the threshold as $|log2FC| > 1$ and adjusted P value < 0.05, we identified 104 DEGs and 4 DElncRNAs (KIAA0125, RUNX1-IT1, LOC100130476, LOC101929272). The heatmap of the DEGs and DElncRNAs showed that the periodontitis clustered separately from the healthy tissues (Fig. 1A-B). At the threshold value of Pearson correlation coefficient greater than 0.5, DElncRNAs and DEGs expressed jointly were predicted and the integrated networks ware visualized. The co-expression between up-regulated DElncRNAs (KIAA0125, RUNX1-IT1, LOC101929272) and DEGs could be seen in Fig. 1C-1E while the co-expression between down-regulated DElncRNAs (LOC100130476) and DEGs could be seen in Fig. 1F. Among them, the positive regulatory relationship between DElncRNAs and DEGs was marked as red, while the negative regulatory relationship was marked as blue.

Immune cells and differentially expressed IRGs in periodontitis

Through the CIBERSORT database, we predicted the abundance of immune cells in the GSE10334 dataset, and plotted the histogram, heatmap, and box map of the corresponding immune cell content (Fig. 2A-C). The results showed that there was a clear difference in immune cell content between normal tissue and periodontitis. In addition, the number of B cells, especially plasma cells, increased in

periodontitis affected tissues. Besides, we drew the corresponding heatmap of the relationship between the abundance values of 22 immune cells (Fig. 2D). Using a cut-of threshold of |log2 FC| > 1 and adjusted P value < 0.05, we identified 26 IRGs (Fig. 2E). In addition, we conducted and visualized a co-expression network between 26 IRGs and 4 DElncRNAs (Fig. 2F). The results showed that 4 DElncRNAs have strong associations with CD19 and CD79A (P < 0.0001), which the markers of B cells (Table 1 and Supplementary Table 1). Therefore, we calculated the Pearson correlation to verify the relationship between the abundance of three types of B cells (B cells naive, B cells memory and plasma cells) and the gene expression of DElncRNAs. The results showed that 4 DElncRNAs were strongly associated with plasma cells (P < 0.0001; Fig. 3), and lncRNA KIAA0125 showed the highest correlation with plasma cells (correlation = 0.7726).

Table 1
The correlation between the expression levels of 4 differentially expressed lncRNAs (DElncRNAs) and the expression levels of CD19 and CD79A.

immuneGene	lncRNA	cor	pvalue	Regulation
CD79A	KIAA0125	0.907940185	1.65E-94	postive
CD19	KIAA0125	0.852454002	5.86E-71	postive
CD79A	RUNX1-IT1	0.725882443	1.06E-41	postive
CD19	RUNX1-IT1	0.675955722	2.49E-34	postive
CD79A	LOC100130476	-0.764481435	1.28E-48	negative
CD19	LOC100130476	-0.724638626	1.69E-41	negative
CD79A	LOC101929272	0.872994613	2.34E-78	postive
CD19	LOC101929272	0.82743604	2.46E-63	postive

Construction of a ceRNA network for periodontitis

The gene expression profiles of periodontitis were integrated to find the differentially expressed lncRNAs, miRNAs and mRNAs in periodontitis, so as to construct ceRNA network, identify the role of ceRNA network in periodontitis and better understand the role of DElncRNAs on mRNAs mediated by miRNAs. The results showed that only 1 DElncRNA (KIAA0125) interacted with 64 DEmiRNAs through the miRcode database (Supplementary Table 2). We searched for differentially expressed mRNAs (DEmRNAs) from 64 DEmiRNAs in the miRDB, TargetScan and miRTarBase databases. Finally we obtained 1 DElncRNA (KIAA0125), 3 DEmiRNAs (miR-449c-5p, miR-125a-5p and miR-125b-5p) and 2 DEmRNAs (BTG2 and CYP24A1) interacting with each other and established the corresponding ceRNA network (Fig. 4).

Identification of key genes by WGCNA analysis

We performed WGCNA analysis on the gene expression profiles of 69 normal tissues and 241 periodontitis tissues to find the modules most relevant to clinical traits and explore the key genes among

them. In this study, we chose the power of β = 13 to construct a scale-free network (Fig. 5A). Finally, we obtained 9 gene co-expression modules by combining dynamic tree cutting (Fig. 5B). After combining the module with clinical traits, we found that the turquoise module was closely related to the periodontitis (P = 8e-38; Fig. 5C), and it also contained the genes BTG2, CYP24A1 and KIAA0125 (Fig. 5C an 5D). In addition, we drew the scatter diagram of GS vs MM in the turquoise module with the periodontitis (correlation = 0.7, P = 1.4e-104) (Fig. 5D).

Gene expression profiles of healthy tissues and periodontitis

We analyzed the mRNA expression levels measured in 1 gingival tissue from periodontitis patient and 2 normal gingival tissues, which divided into normal gingival group 1 (N1), normal gingival group 2 (N2) and periodontitis group (CP). The clinical characteristics of the periodontitis patient and normal people can be referred to Supplementary Table 3. Through the RNA sequence data, we found that the gene expression patterns showed significantly different expression levels among periodontitis and healthy tissues. The differential scatter diagrams in Fig. 6A was created to identify differences among mRNAs using the edgeR algorithm (fold changes > 2 and adjusted P value < 0.05). The clustered heatmap and Venn diagram of DEGs are shown in Figs. 6B and 6C. There were 3461 differentially expressed genes between N1 and CP, among which 1050 genes were up-regulated and 2411 genes were down-regulated (Supplementary Table 4). There were 2318 differentially expressed genes between N2 and CP groups, among which there were 1710 up-regulated genes and 608 down-regulated genes (Supplementary Table 5). In total, there were 808 identical genes in the two groups, including gene CYP24A1. Figure 1A have shown a positive regulatory relationship between lncRNA KIAA0125 and CYP24A1. Therefore, we further verified the expression and functional relationship between CYP24A1 and KIAA0125 in periodontitis.

Validation of Immune-related lncRNA KIAA0125 and CYP24A1 in gingival tissues with periodontitis

For further verification, we used qRT-PCR to measure the expression of KIAA0125, CYP24A1, CD19, CD79A, IL1B and IL6 in 13 periodontitis gingival tissues and 12 normal tissues and the clinical characteristics of all patients were shown in Supplementary Table 6. The KIAA0125 and CYP24A1 gene expression were significantly up-regulated in periodontitis gingival tissues compared with healthy tissues (P = 0.0024, P < 0.0001; Fig. 7A and 7B). Furthermore, as shown in Fig. 7C-7D, CD19 and CD79A were also over-expressed in periodontitis compared to the normal tissues (P < 0.001). In addition, the significant increase of IL1B and IL6 also indicated the higher inflammation level in the periodontitis group (P < 0.0001; Fig. 7E and 7F). The above results suggested that KIAA0125 was positively regulated with CD19 and CD79A, so we analyzed the correlation between the expression levels of CD79A and CD19 and the expression levels of KIAA0125 and CYP24A. From Fig. 7G-7H, we found KIAA0125 have the highest correlation with CD19 and CD79A (correlation = 0.8760, P = 0.0002; correlation = 0.6953, P = 0.0121). In addition, the results also showed that CYP24A1 was also highly correlated with CD19 and CD79A

(correlation = 0.8115, P = 0.0014; correlation = 0.7032, P = 0.0107; Fig. 7I and 7J). Next, we analyzed the correlations between the expression of KIAA0125 and CYP24A1 and clinicopathological features in all the patients respectively (Fig. 8A-8H). In addition to the gingival index (GI), the other clinical features such as plaque index (PLI), probing depth (PD) and clinical attachment level (CAL) were significantly correlated with the expression of KIAA0125 and CYP24A1 ($P < 0.05$). Especially, the expression of KIAA0125 was significantly correlated with PD (correlation = 0.9361, $P < 0.0001$; Fig. 8C).

Validation the synergistic effect of KIAA0125 and CYP24A1

CCK-8 was used to detect the change of hPDLCs proliferation rate under the influence of different concentrations of LPS, and the results showed that there were statistically significant differences between the experimental groups and the control group. The low concentration of LPS promoted the proliferation of hPDLCs, which reached the peak at 1 μg/ml, and then the proliferation rate decreased with the increase of LPS concentration (Supplementary Fig. 1). Therefore, the concentration of LPS used in the test was finally determined to be 1 μg/mL. The results of qRT-PCR showed that under LPS stimulation, the relative expression levels of KIAA0125, CYP24A1, CD19, CD79A, IL1B and IL6 were increased. Compared with the control group, KIAA0125, CD79A and IL1B showed a statistically significant difference ($P < 0.05$; Fig. 9).

CYP24A1 is a key enzyme in vitamin D metabolism, which enables 1,25D to produce extremely inactive metabolites, thus maintaining stable blood calcium concentrations. To clarify the effect of 1,25D on hPDLCs in an inflammatory environment, we added 10 nM 1,25D to treat hPDLCs for 24 hours. The results showed that the relative expression levels of inflammatory factors IL1B and IL6 decreased compared with the LPS group, and the difference of IL1B was statistically significant ($P < 0.001$; Fig. 10E). In addition, the expression levels of CD19 and CD79A also decreased compared with the LPS group, but the results were not statistically significant. Contrary to this result, the expression levels of KIAA0125 and CYP24A1 increased significantly compared with the LPS group, especially the increase of KIAA0125 was statistically significant ($P < 0.05$; Fig. 10A).

The cytochrome P450 inhibitor ketoconazole was used to block the effect of 24-hydroxylase (encoded by CYP24A1 gene) on 1,25D catabolic activity. Therefore, we investigated the possibility that ketoconazole could suppress the response of hPDLCs to 1,25D in the inflammatory environment. The results showed that 10 μM ketoconazole plus 10 nM 1,25D and 1 μg/mL LPS significantly increased the level of CYP24A1 mRNA transcription in hPDLCs compared to LPS group ($P < 0.001$; Fig. 10B). With the increase of CYP24A1, we found that KIAA0125, CD19, CD79A, IL1B and IL6 were also increased, especially the increase of KIAA0125 and IL1B was statistically significant ($P < 0.01$; $P < 0.05$; Fig. 10A and 10E). In contrast, 100 μM ketoconazole combined with 1,25D (10 nM) and 1 μg/mL LPS reduced the expression of CYP24A1 in hPDLCs, relative to the cells treated with 10 μM ketoconazole ($P < 0.001$; Fig. 10B). With the decrease of CYP24A1, the expression levels of inflammatory cytokines IL1B and IL6 were significantly decreased compared with the LPS group ($P < 0.001$; $P < 0.01$; Fig. 10E and 10F). In addition, the expression levels of KIAA0125, CD19, and CD79A were also decreased compared to hPDLCs treated with

10 μM ketoconazole ($P < 0.01$; Fig. 10A, 10C and 10D). Through the above experiments, we found that the expression trend of KIAA0125 and CYP24A1 was consistent in the inflammatory environment.

Discussion

Periodontitis is a common and frequent occurring disease in human oral cavity, which can cause gingival inflammation, alveolar bone resorption and teeth loosening and falling out. Plaque biofilm is the initiating factor that causes periodontitis, and excessive immune inflammatory response of the host also plays an important role in the occurrence and development of periodontitis [20]. At present, some studies have confirmed that lncRNA may change the function of periodontal related cells in the microenvironment of periodontitis. Li et al. Found lncRNA SNHG1 associated with osteoblastic dysfunction in periodontitis can regulate the osteogenic differentiation of inflammatory periodontal ligament stem cells through EZH2-mediated H3K27me3 methylation of KLF2 promotor [21]. In this study, 4 DElncRNAs (KIAA0125, Runx1-IT1, LOC100130476, LOC101929272) were screened out from the dataset GSE10334. The results showed that the expressions of KIAA0125, Runx1-IT1, and LOC10191929272 were significantly increased in periodontitis, while the expressions of LOC100130476 were decreased.

Next, we investigated the infiltration of immune cells in the periodontitis group and the normal group, and found that plasma cell infiltration was dominant. Besides, we found that four DElncRNAs have high correlation to B cell surface Markers CD19 and CD79A. qRT-PCR results also showed that CD19 and CD79A were up-regulated in periodontitis. Some studies have shown that T lymphocytes and B lymphocytes are dominant in the chronic inflammatory period of periodontitis, and up to 50% of B lymphocytes were detected in gingival tissue [22]. B cells/plasma cells play a protective role in periodontitis. The antibody response against bacteria is beneficial to control the imbalance of microbial flora in the periodontal pocket and prevent bacteria from entering the connective tissue of the gingiva, thus limiting the inflammation and disease. While B cells secrete TNF-α, IL-1β, IL-17, MMPS or plasma cells secrete IgA, IgG, IgM and other antibodies to kill pathogens, they also promote the expression of RANKL to activate osteoclasts and accelerate alveolar bone absorption [23, 24]. Studies have shown that B lymphocytes are one of the main sources of RANKL in periodontal lesion tissues. Up to 90% of B lymphocytes in inflammatory tissues of periodontitis express RANKL [25]. Currently, Suzuki et al. identified CD19 and CD79A as the molecular biomarker candidates and pathogenesis of chronic periodontitis [26]. The above evidence suggested that B lymphocytes play an important role in the development of periodontitis.

In order to explore the regulatory network of DElncRNAs, we constructed the ceRNA network and a total of 1 lncRNA (KIAA0125), 3 miRNAs (miR-449c-5p, miR-125a-5p and miR-125b-5p) and 2 mRNAs (CYP24A1, BTG2) were involved in establishing the ceRNA network for periodontitis. KIAA0125 is a long non-coding RNA gene, which is located on chromosome 14q32.33. KIAA0125 was first reported in 1995, the mechanism of which under human physiological and pathological conditions has been rarely explored [27]. Studies have found that lncRNA KIAA0125 was down-regulated in colorectal cancer and inhibited epithelial-mesenchymal transition (EMT) through Wnt/β-catenin signaling [28]. However, Diniz et al.

detected that the expression level of KIAA0125 transcript in the ameloblastoma group was higher than that of dental follicles, which may be involved in the pathobiological process of ameloblastoma [29]. Few studies on KIAA0125 have been conducted in periodontitis. However, Guzeldemir-akcakanat et al. found that KIAA0125 was highly expressed in the chronic periodontitis group by whole-genome Transcriptomic [30]. The specific mechanism of KIAA0125 involved in the pathogenic process of periodontitis needs to be further explored.

Through WGCNA analysis and transcriptomic sequencing results, we further found that CYP24A1 was the key mRNA. 1,25D is the main bioactive form of vitamin D, and its role in the prevention and treatment of osteoporosis, diabetes and periodontitis has been attracting people's attention. The main role of 1,25D is to regulate calcium and phosphorus metabolism. However, in recent years, as an immunomodulator, its role in anti-inflammatory and immunomodulatory has become a focus of research, especially its role in innate immunity. 1,25D can up-regulate the expression of antimicrobial peptides, urge phagocytes to kill pathogenic microorganisms, down-regulate the expression of inflammatory factors, and reduce the inflammatory response [31]. Vitamin D 24-hydroxylase can add hydroxyl to the 24-bit carbon atom of 1,25D, thus greatly reducing the activity. It is an inhibitor of 1,25D activity in vivo and negatively regulates the biological effects of 1,25D, the gene encoded by which is CYP24A1 [32]. Liu et al. found that the mRNA expression of CYP24A1 and RANKL in human gingival fibroblasts (hGF) and PDLCs significantly increased after treatment 1,25D [33]. In addition, most studies suggested that the abnormal expression of CYP24A1 leads to excessive or insufficient 1,25D, which is associated with the occurrence and development of most cancers. Studies have found that the risk of colorectal cancer was negatively correlated with the status of vitamin D in patients, and vitamin D supplementation can reduce the incidence of colorectal cancer. The expression level of CYP24A1 increased during the occurrence of colorectal cancer, and the higher the level of CYP24A1, the higher the malignancy of colorectal cancer. At the same time, the expression level of Ki-67, a marker for cancer cell proliferation, also increased, suggesting that the overexpression of CYP24A1 reduced the local practicability and anti-tumor effect of 1,25D [34]. Wang et al. demonstrated that knockdown of CYP24A1 can aggravate 1,25D to suppress EMT, proliferation and invasion, increase the expression of E-cadherin, and reduce the expression of N-cadherin, Vimentin, β-catenin and Snail in mouse ovarian epithelial cells [35]. These above findings suggested that inhibition of CYP24A1 may activate the vitamin D pathway in prevention and treatment of diseases.

qRT-PCR results by us showed that both KIAA0125 and CYP24A1 were highly expressed in periodontitis and correlated with the clinical characteristics of PLI, PD and CAL. In addition, we found that both KIAA0125 and CYP24A1 were positively correlated with CD19 and CD79A expression levels. When treated with 1 μg/mL LPS for 24 h, KIAA0125 and CYP24A1 expression in hPDLCs were increased, and the results of KIAA0125 were statistically significant. Next, we explored the effects on the expression levels of key genes in an inflammatory environment. When treated with 1 μg/mL LPS and 10 nM 1,25D, the expressions of KIAA0125 and CYP24A1 were significantly increased, while the inflammatory factors IL1B and IL6 were relatively decreased, suggesting that 1,25D could alleviate inflammation. When we added low-dose ketoconazole, we found that the expression levels of KIAA0125 and CYP24A1 were further

increased. With the increase of the expression levels, CD19, CD79A, IL1B and IL6 were relatively increased, which also indicated that CYP24A1 and KIAA0125 could reduce the anti-inflammatory effect of 1,25D. When we used high doses of ketoconazole, KIAA0125 and CYP24A1 were significantly inhibited, and as their expression decreased, so did the expression of inflammatory factors. Through vitro experiments, we found that 1,25D could alleviate the inflammation of LPS-induced hPDLCs, while the increased expression of KIAA0125 and CYP24A1 would antagonize the anti-inflammatory effect.

This study has some limitations. First of all, we screened out the key gene CYP24A1 through WGCNA analysis and transcriptional sequencing and made subsequent verification, but we did not conduct subsequent experiments on BTG2 and miRNAs in the ceRNA network. In addition, the specific mechanism of the co-expression of KIAA0125 and CYP24A1 remains to be further explored.

Conclusions

Through this study, we identified differentially expressed immune related lncRNA KIAA0125 may have important significance in the immune microenvironment and pathogenesis of periodontitis. In addition, we found that KIAA0125 have the closely correlation with vitamin D metabolism related gene CYP24A1 in periodontitis, which needs to be further explored the specific mechanism by later experiments.

Declarations

Acknowledgements

Not applicable.

Funding

The authors declare that there is no funding for the research.

Availability of data and materials

The datasets generated and analyzed during the current study are available in GSE10334 (https://www.ncbi.nlm.nih.gov/geo/query/acc.cgi?acc=GSE10334) and GSE16134 (https://www.ncbi.nlm.nih.gov/geo/query/acc.cgi?acc=GSE16134).

Authors' contributions

YL, RXL, YW and XJD mainly performed experiments and data analysis. YL, RXL and YW wrote the manuscript. YL, RXL, YW, CJG and XJD designated all experiments in this study. All authors contributed to the critical review of the manuscript.

Ethics approval and consent to participate

The tissue collection process, cell culture, and RNA isolation were conducted according to the principles expressed in the Declaration of Helsinki and approved by Ethical Committee at Zhongshan Hospital (NO. B2020-128R). Written informed consent for the gingival tissues used in this study was obtained from all patients prior to surgery.

Consent for publication

Not applicable.

Competing interests

The authors declare that they have no competing interests.

References

1. Papapanou PN, Sanz M, Buduneli N, Dietrich T, Feres M, Fine DH, Flemmig TF, Garcia R, Giannobile WV, Graziani F <bi>et al</bi>: Periodontitis: Consensus report of workgroup 2 of the 2017 World Workshop on the Classification of Periodontal and Peri-Implant Diseases and Conditions. *J Periodontol* 2018, 89 Suppl 1:S173-s182.
2. Okui T, Aoki Y, Ito H, Honda T, Yamazaki K: The presence of IL-17+/FOXP3 + double-positive cells in periodontitis. J Dent Res 2012, 91(6):574–579.
3. Ye M, Zhang J, Wei M, Liu B, Dong K: Emerging role of long noncoding RNA-encoded micropeptides in cancer. *Cancer Cell Int* 2020, 20:506.
4. Kotzin JJ, Spencer SP, McCright SJ, Kumar DBU, Collet MA, Mowel WK, Elliott EN, Uyar A, Makiya MA, Dunagin MC <bi>et al</bi>: The long non-coding RNA Morrbid regulates Bim and short-lived myeloid cell lifespan. *Nature* 2016, 537(7619):239–243.
5. Shin TJ, Lee KH, Cho JY: Epigenetic Mechanisms of LncRNAs Binding to Protein in Carcinogenesis. *Cancers (Basel)* 2020, 12(10).
6. Huang X, Chen K: Differential Expression of Long Noncoding RNAs in Normal and Inflamed Human Dental Pulp. *J Endod* 2018, 44(1):62–72.
7. Huang N, Li C, Sun W, Wu J, Xiao F: Long non-coding RNA TUG1 participates in LPS-induced periodontitis by regulating miR-498/RORA pathway. *Oral Dis* 2020.
8. Jin T, Guo Y, Huang Z, Zhang Q, Huang Z, Zhang Y, Huang Z: Vitamin D inhibits the proliferation of Oral Squamous Cell Carcinoma by suppressing lncRNA LUCAT1 through the MAPK pathway. *J Cancer* 2020, 11(20):5971–5981.
9. Diboun I, Wernisch L, Orengo CA, Koltzenburg M: Microarray analysis after RNA amplification can detect pronounced differences in gene expression using limma. *BMC Genomics* 2006, 7:252.
10. Shannon P, Markiel A, Ozier O, Baliga NS, Wang JT, Ramage D, Amin N, Schwikowski B, Ideker T: Cytoscape: a software environment for integrated models of biomolecular interaction networks. Genome Res 2003, 13(11):2498–2504.

11. Newman AM, Liu CL, Green MR, Gentles AJ, Feng W, Xu Y, Hoang CD, Diehn M, Alizadeh AA: Robust enumeration of cell subsets from tissue expression profiles. *Nat Methods* 2015, 12(5):453–457.
12. Bhattacharya S, Dunn P, Thomas CG, Smith B, Schaefer H, Chen J, Hu Z, Zalocusky KA, Shankar RD, Shen-Orr SS <bi>et al</bi>: ImmPort, toward repurposing of open access immunological assay data for translational and clinical research. *Sci Data* 2018, 5:180015.
13. Jeggari A, Marks DS, Larsson E: miRcode: a map of putative microRNA target sites in the long non-coding transcriptome. *Bioinformatics* 2012, 28(15):2062–2063.
14. Agarwal V, Bell GW, Nam JW, Bartel DP: Predicting effective microRNA target sites in mammalian mRNAs. *Elife* 2015, 4.
15. Chou CH, Shrestha S, Yang CD, Chang NW, Lin YL, Liao KW, Huang WC, Sun TH, Tu SJ, Lee WH <bi>et al</bi>: miRTarBase update 2018: a resource for experimentally validated microRNA-target interactions. *Nucleic Acids Res* 2018, 46(D1):D296-d302.
16. Wong N, Wang X: miRDB: an online resource for microRNA target prediction and functional annotations. *Nucleic Acids Res* 2015, 43(Database issue):D146-152.
17. Kunowska N, Rotival M, Yu L, Choudhary J, Dillon N: Identification of protein complexes that bind to histone H3 combinatorial modifications using super-SILAC and weighted correlation network analysis. *Nucleic Acids Res* 2015, 43(3):1418–1432.
18. Li B, Dewey CN: RSEM: accurate transcript quantification from RNA-Seq data with or without a reference genome. *BMC Bioinformatics* 2011, 12:323.
19. Robinson MD, McCarthy DJ, Smyth GK: edgeR: a Bioconductor package for differential expression analysis of digital gene expression data. *Bioinformatics* 2010, 26(1):139–140.
20. Kinane DF, Stathopoulou PG, Papapanou PN: Periodontal diseases. *Nat Rev Dis Primers* 2017, 3:17038.
21. Li Z, Guo X, Wu S: Epigenetic silencing of KLF2 by long non-coding RNA SNHG1 inhibits periodontal ligament stem cell osteogenesis differentiation. *Stem Cell Res Ther* 2020, 11(1):435.
22. Kanzaki H, Makihira S, Suzuki M, Ishii T, Movila A, Hirschfeld J, Mawardi H, Lin X, Han X, Taubman MA <bi>et al</bi>: Soluble RANKL Cleaved from Activated Lymphocytes by TNF-α-Converting Enzyme Contributes to Osteoclastogenesis in Periodontitis. *J Immunol* 2016, 197(10):3871–3883.
23. Gümüş P, Nizam N, Lappin DF, Buduneli N: Saliva and serum levels of B-cell activating factors and tumor necrosis factor-α in patients with periodontitis. *J Periodontol* 2014, 85(2):270–280.
24. Martinho FC, Teixeira FF, Cardoso FG, Ferreira NS, Nascimento GG, Carvalho CA, Valera MC: Clinical Investigation of Matrix Metalloproteinases, Tissue Inhibitors of Matrix Metalloproteinases, and Matrix Metalloproteinase/Tissue Inhibitors of Matrix Metalloproteinase Complexes and Their Networks in Apical Periodontitis. *J Endod* 2016, 42(7):1082–1088.
25. Kawai T, Matsuyama T, Hosokawa Y, Makihira S, Seki M, Karimbux NY, Goncalves RB, Valverde P, Dibart S, Li YP <bi>et al</bi>: B and T lymphocytes are the primary sources of RANKL in the bone resorptive lesion of periodontal disease. *Am J Pathol* 2006, 169(3):987–998.

26. Suzuki A, Horie T, Numabe Y: Investigation of molecular biomarker candidates for diagnosis and prognosis of chronic periodontitis by bioinformatics analysis of pooled microarray gene expression datasets in Gene Expression Omnibus (GEO). *BMC Oral Health* 2019, 19(1):52.
27. Nagase T, Seki N, Tanaka A, Ishikawa K, Nomura N: Prediction of the coding sequences of unidentified human genes. IV. The coding sequences of 40 new genes (KIAA0121-KIAA0160) deduced by analysis of cDNA clones from human cell line KG-1. *DNA Res* 1995, 2(4):167–174, 199–210.
28. Yang Y, Zhao Y, Hu N, Zhao J, Bai Y: lncRNA KIAA0125 functions as a tumor suppressor modulating growth and metastasis of colorectal cancer via Wnt/β-catenin pathway. *Cell Biol Int* 2019, 43(12):1463–1470.
29. Diniz MG, França JA, Vilas-Boas FAS, de Souza FTA, Calin GA, Gomez RS, de Sousa SF, Gomes CC: The long noncoding RNA KIAA0125 is upregulated in ameloblastomas. *Pathol Res Pract* 2019, 215(3):466–469.
30. Guzeldemir-Akcakanat E, Alkan B, Sunnetci-Akkoyunlu D, Gurel B, Balta VM, Kan B, Akgun E, Yilmaz EB, Baykal AT, Cine N <bi>et al</bi>: Molecular signatures of chronic periodontitis in gingiva: A genomic and proteomic analysis. *J Periodontol* 2019, 90(6):663–673.
31. Christakos S, Dhawan P, Liu Y, Peng X, Porta A: New insights into the mechanisms of vitamin D action. *J Cell Biochem* 2003, 88(4):695–705.
32. Luo W, Yu WD, Ma Y, Chernov M, Trump DL, Johnson CS: Inhibition of protein kinase CK2 reduces Cyp24a1 expression and enhances 1,25-dihydroxyvitamin D(3) antitumor activity in human prostate cancer cells. *Cancer Res* 2013, 73(7):2289–2297.
33. Liu K, Meng H, Hou J: Characterization of the autocrine/paracrine function of vitamin D in human gingival fibroblasts and periodontal ligament cells. *PLoS One* 2012, 7(6):e39878.
34. Horváth HC, Lakatos P, Kósa JP, Bácsi K, Borka K, Bises G, Nittke T, Hershberger PA, Speer G, Kállay E: The candidate oncogene CYP24A1: A potential biomarker for colorectal tumorigenesis. *J Histochem Cytochem* 2010, 58(3):277–285.
35. Wang P, Xu J, You W, Hou Y, Wang S, Ma Y, Tan J, Zhang Z, Hu W, Li B: Knockdown of CYP24A1 Aggravates 1α,25(OH)(2)D(3)-Inhibited Migration and Invasion of Mouse Ovarian Epithelial Cells by Suppressing EMT. *Front Oncol* 2020, 10:1258.

Figures

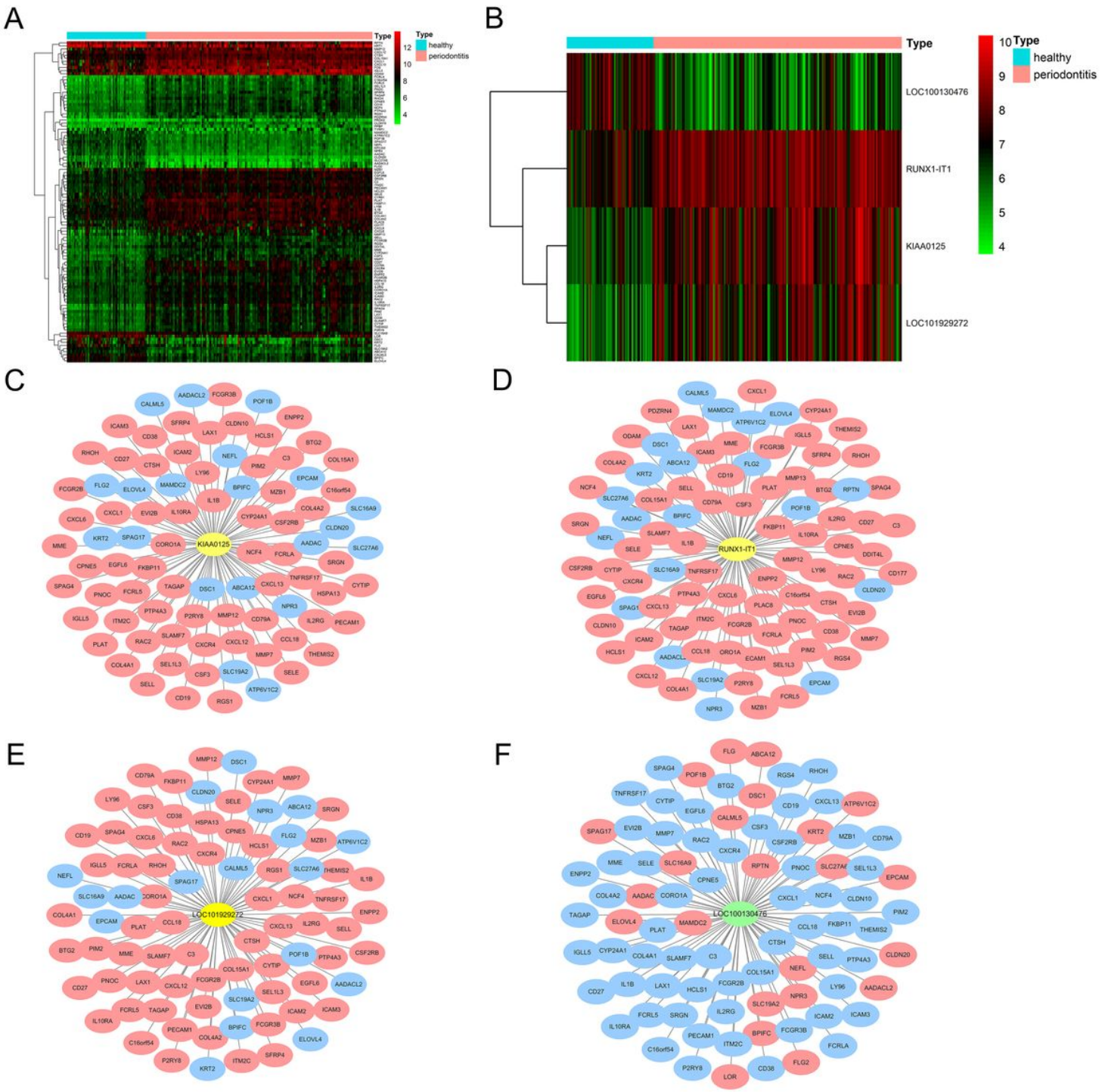

Figure 1

Identification of differentially expressed genes (DEGs) and differentially expressed lncRNAs (DElncRNAs) in periodontitis. (A) DEGs between periodontitis and healthy tissues. (B) DElncRNAs between periodontitis and healthy tissues. (C-E) Integrated network of significantly up-regulated DElncRNAs and DEGs. (F) Integrated network of the significantly down-regulated DElncRNA and DEGs.

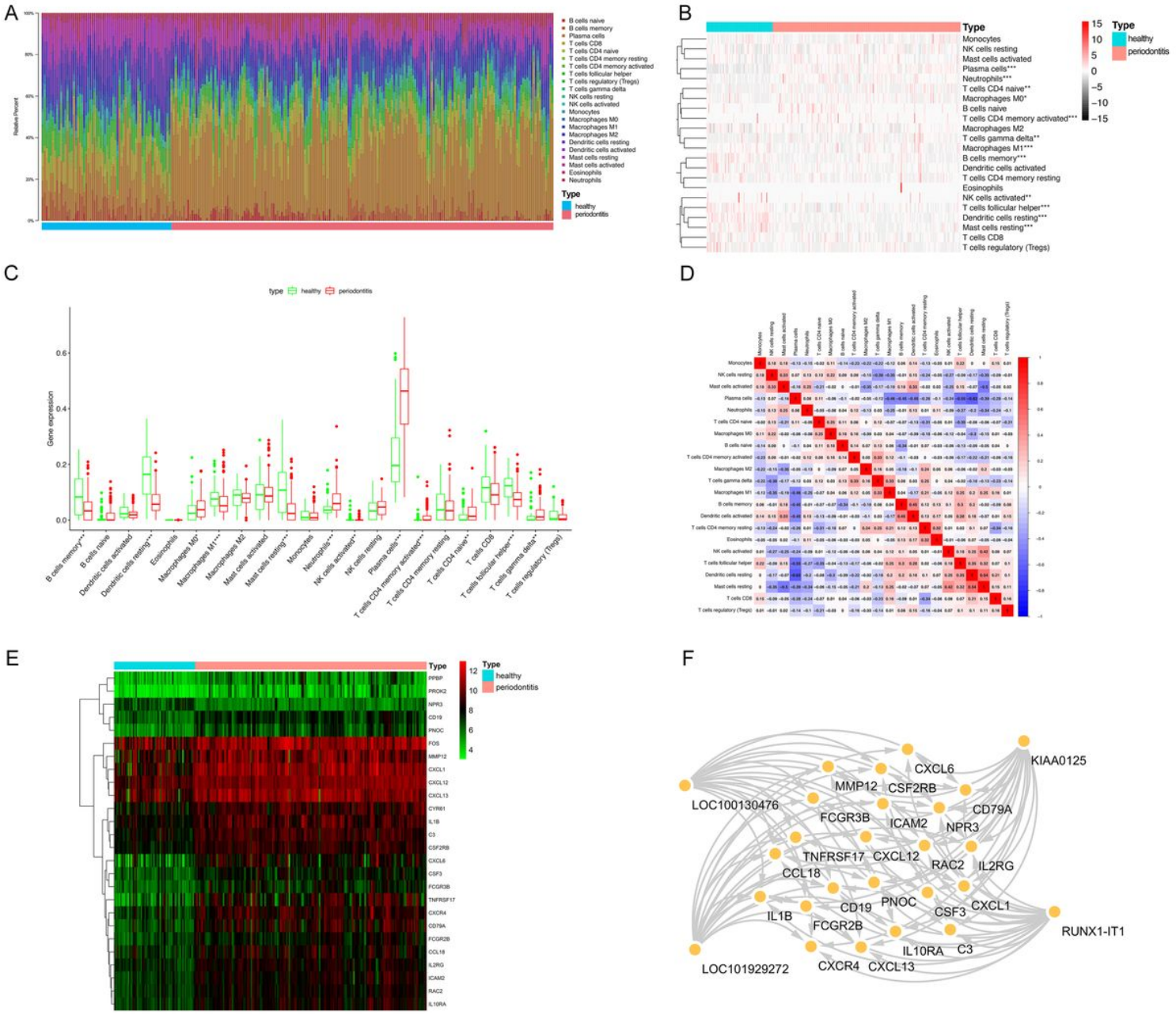

Figure 2

Immune cells and differentially expressed immune-related genes (IRGs) in periodontitis and healthy tissues. (A) Composition of infiltrating immune cells in periodontitis and healthy tissues. (B) Heatmap of the gene expression of immune cell subpopulations. (C) The fraction of infiltrating immune cells in periodontitis and normal tissues. (D) The correlation heatmap between each immune cell. (E) Differentially expressed immune-related genes (IRGs) between periodontitis and normal tissues. (F) Integrated network of significantly differentially expressed lncRNAs (DElncRNAs) and IRGs.

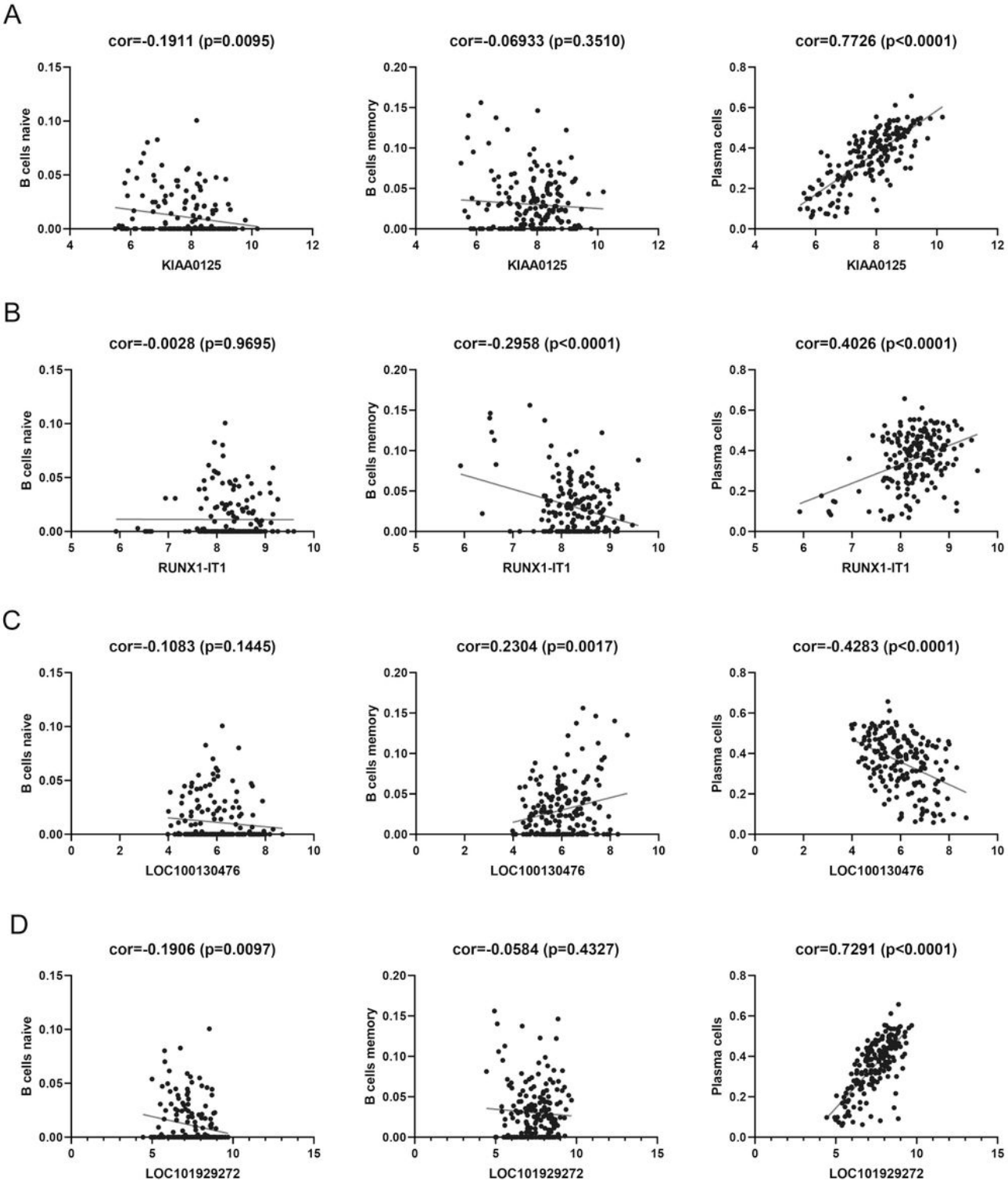

Figure 3

Relationships between the gene expression of differentially expressed lncRNAs (DElncRNAs) and infiltration abundance of three types of B cells. (A) B cells naive; (B) B cells memory; (C) plasma cells.

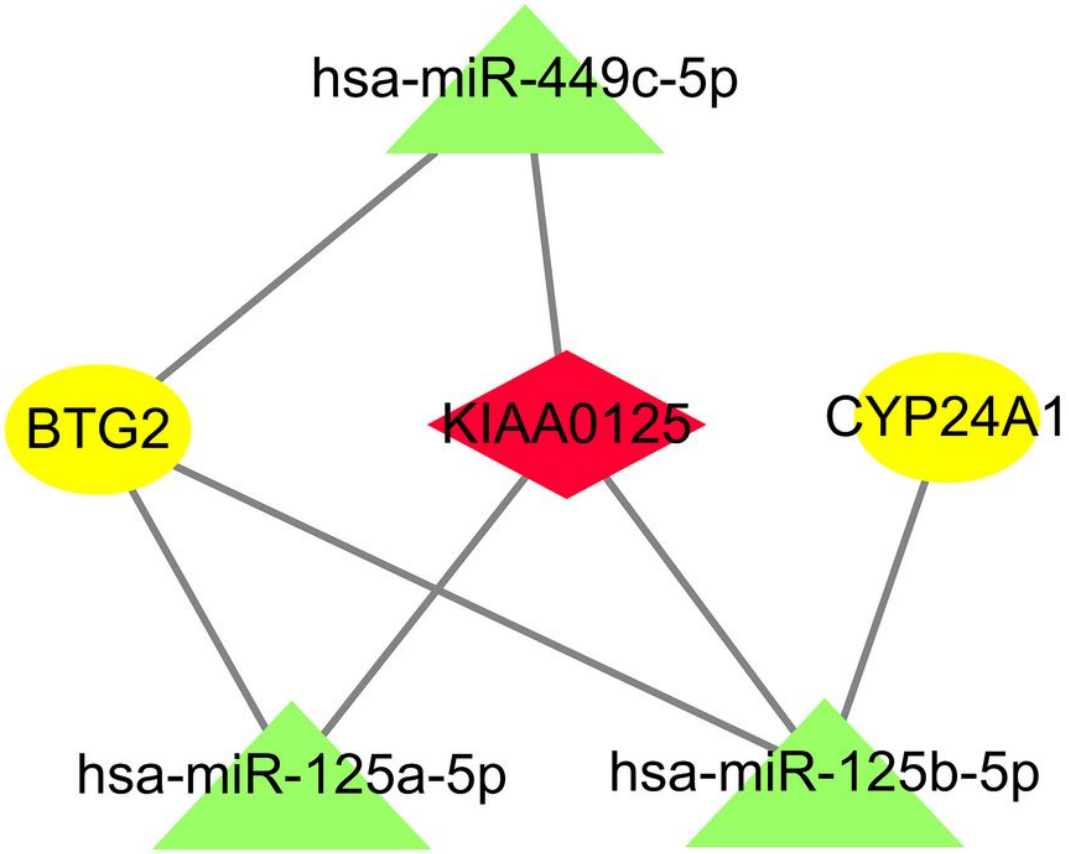

Figure 4

Map of the immune-related lncRNA-miRNA-mRNA network generated using Cytoscape software. Note: The designations employed and the presentation of the material on this map do not imply the expression of any opinion whatsoever on the part of Research Square concerning the legal status of any country, territory, city or area or of its authorities, or concerning the delimitation of its frontiers or boundaries. This map has been provided by the authors.

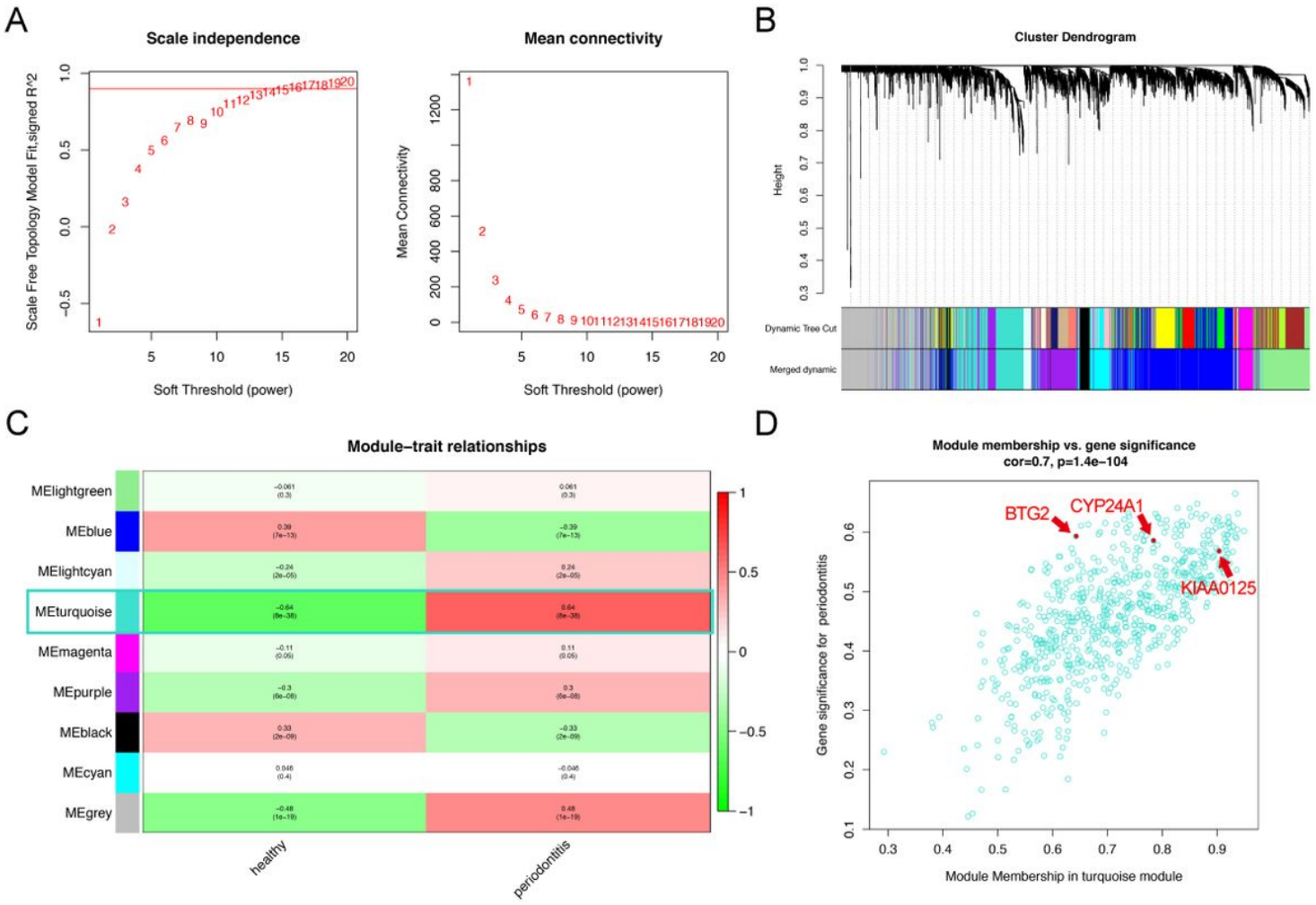

Figure 5

Identification of key genes by weighted gene co-expression network analysis (WGCNA) and the turquoise module containing KIAA0125, CYP24A1 and BTG2. (A) The scale independence and the mean connectivity of the WGCNA analysis of periodontitis. (B) Clustering dendrograms and modules identified by WGCNA. (C) Correlation between module eigengenes and clinical traits. (D) The scatter diagram of gene significance (GS) vs module membership (MM) in the turquoise module of periodontitis. KIAA0125, CYP24A1 and BTG2 has been highlighted in red dots. The cutoff of turquoise module membership = 0.916, 0.643, 0.784, respectively. The cutoff of gene significance for periodontitis = 0.559, 0.593, 0.585 respectively.

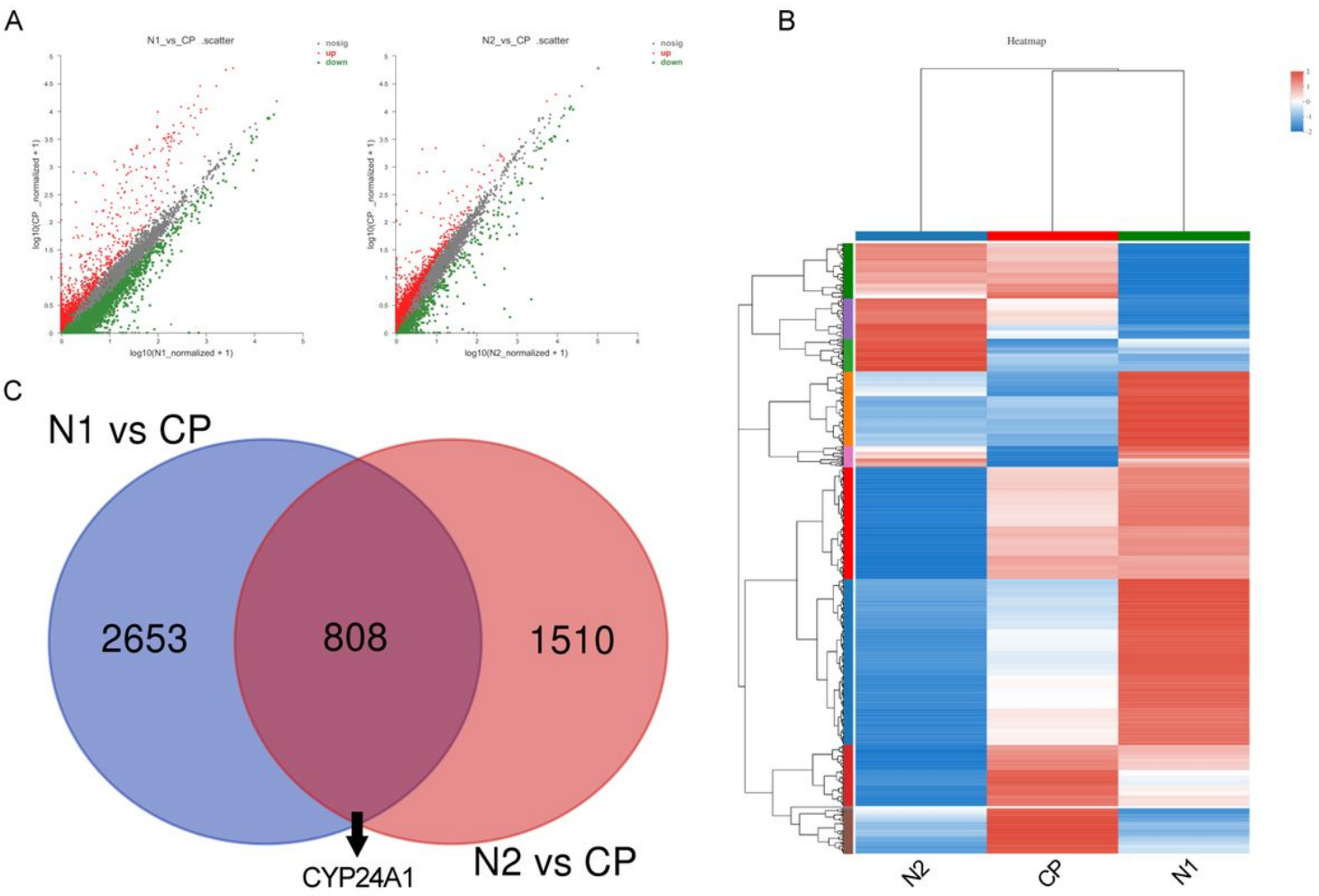

Figure 6

Gene expression profiles of healthy tissues and periodontitis. (A) The differential scatter diagrams of mRNA expression levels between normal gingival group 1 (N1) and periodontitis group (CP) (left) and normal gingival group 2 (N2) and periodontitis group (CP) (right). (B) Heatmap of differentially expressed mRNAs. Red represents up-regulated genes while blue represents down-regulated genes. (C) Venn diagram of differentially expressed mRNAs (adjusted $P < 0.05$; fold change > 2.0).

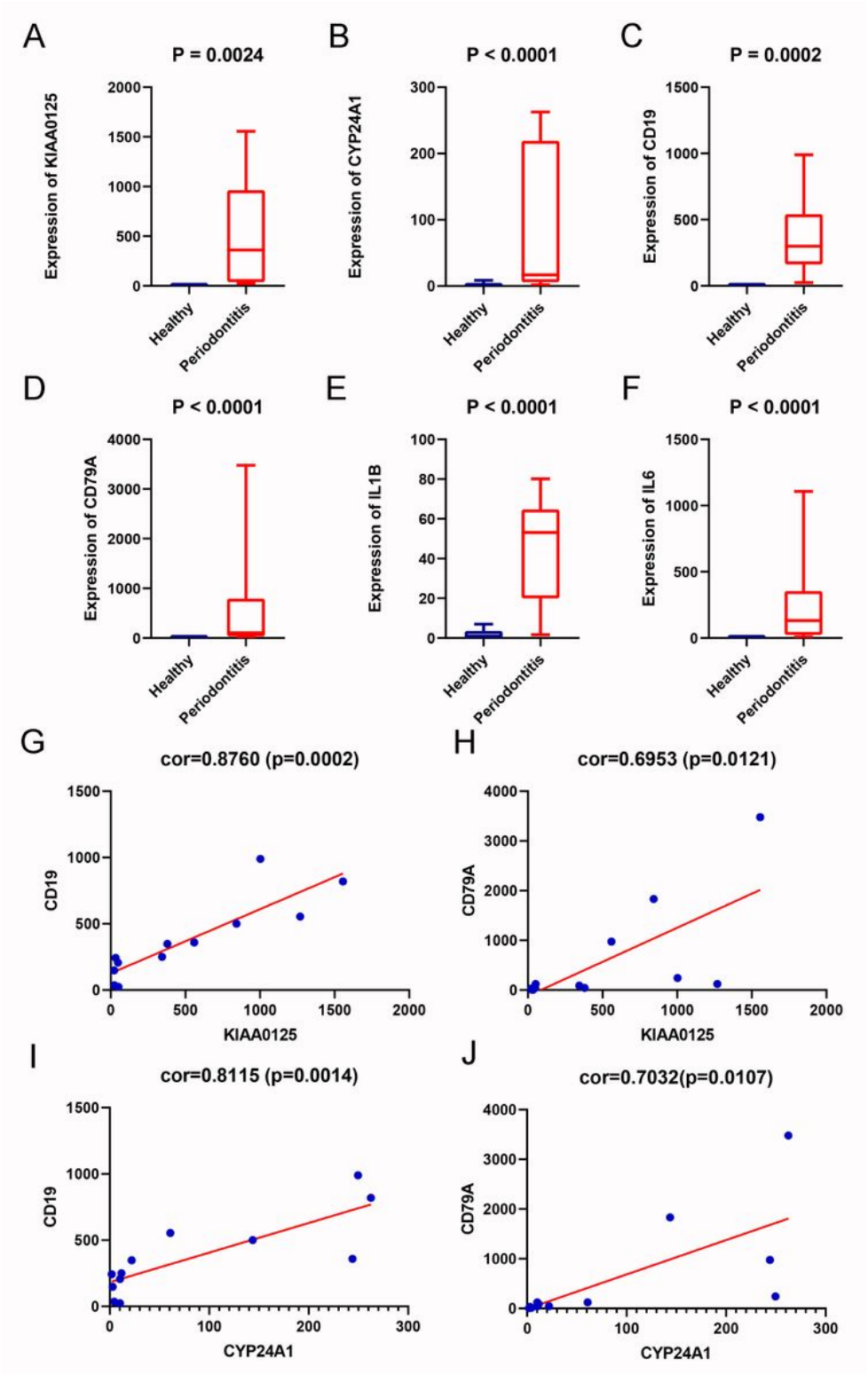

Figure 7

The relative expression level of KIAA0125 (A), CYP24A1 (B), CD19 (C), CD79A (D), IL1B (E) and IL6 (F) in periodontitis gingival tissues compared with healthy tissues. The correlation between the expression levels of KIAA0125 (G-H) and CYP24A1 (I-J) and the expression levels of CD19 and CD79A.

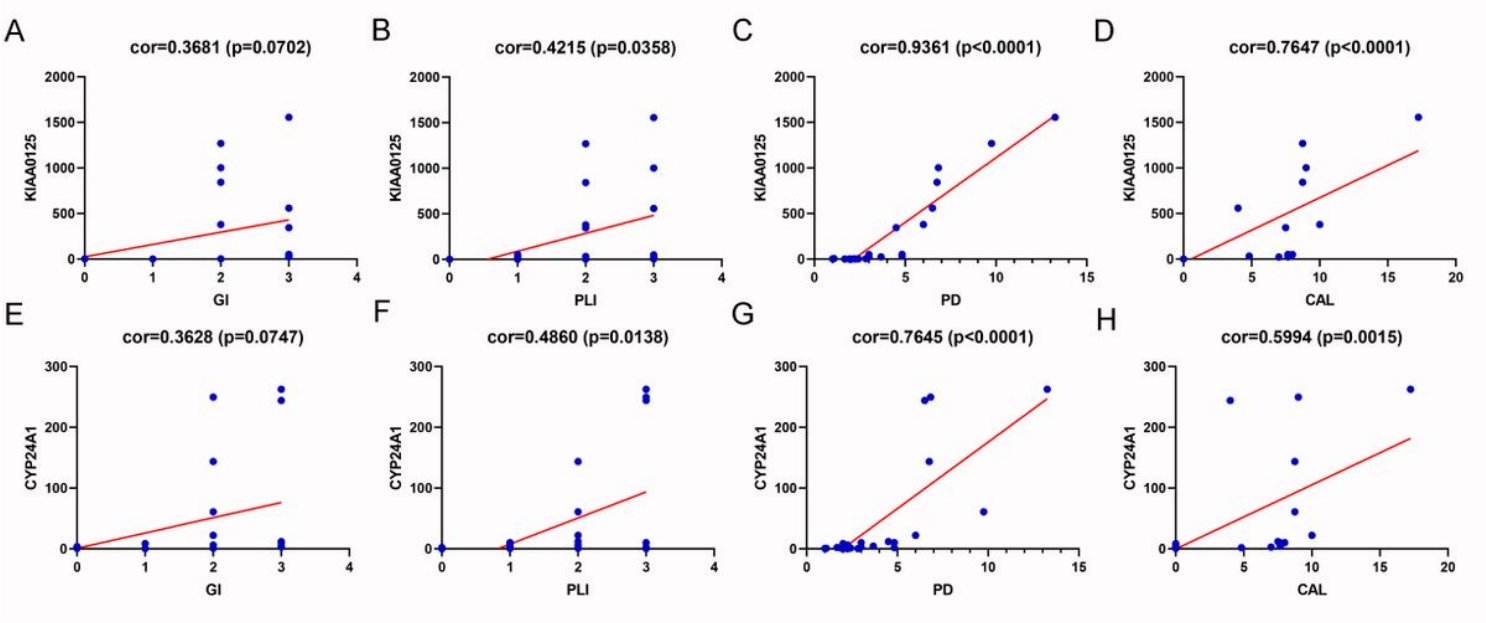

Figure 8

The correlation of KIAA0125 (A-D) and CYP24A1 (E-F) expression levels and clinicopathological features (gingival index (GI), plaque index (PLI), probing depth (PD) and clinical attachment level (CAL)) of periodontitis patients.

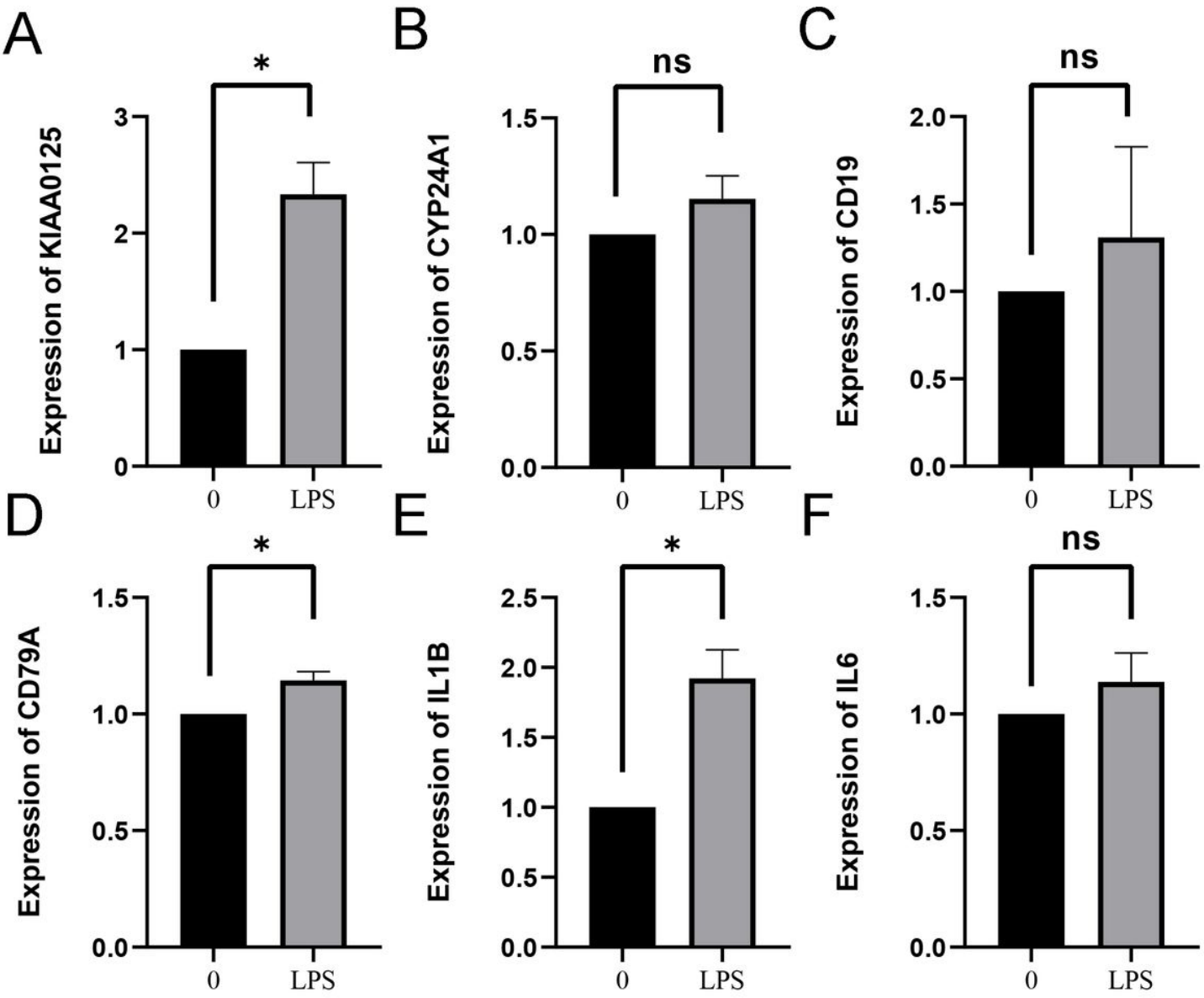

Figure 9

Quantitative real-time PCR determination of KIAA0125 (A), CYP24A1 (B), CD19 (C), CD79A (D), IL1B (E) and IL6 (F) mRNA levels in hPDLCs treated with vehicle and 1 μg/mL LPS. *P < 0.05, ns: no significance.

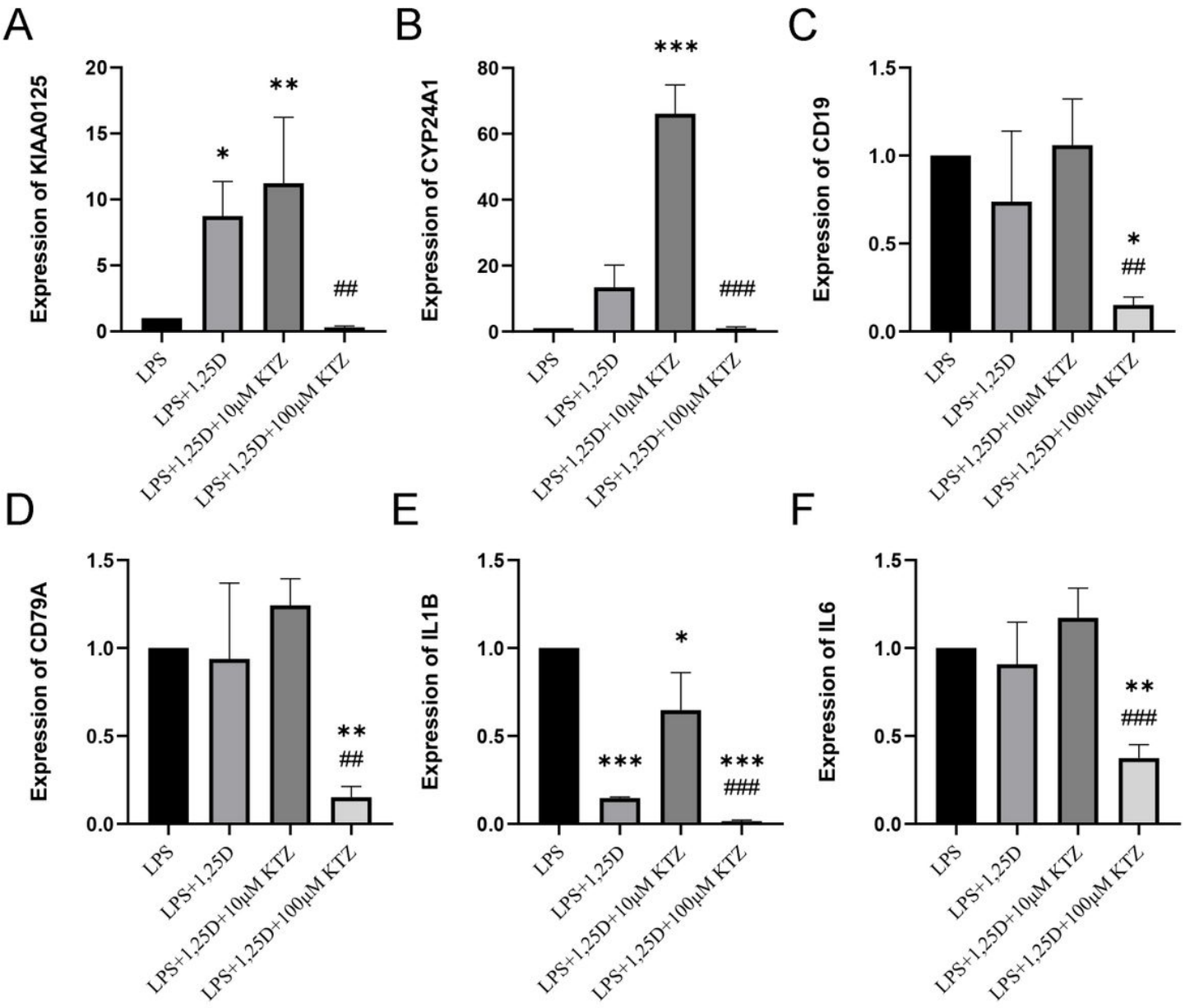

Figure 10

Quantitative real-time PCR determination of KIAA0125 (A), CYP24A1 (B), CD19 (C), CD79A (D), IL1B (E) and IL6 (F) mRNA levels in hPDLCs treated with 1 μg/mL LPS, 1 μg/mL LPS in combination with 10 nM 1,25D, 1 μg/mL LPS in combination with 10 nM 1,25D and 10 μM ketoconazole, and 1 μg/mL LPS in combination with 10 nM 1,25D and 100 μM ketoconazole for 24 hours. *Comparison with baseline level of LPS group; #Comparison with baseline levels of 10 μM ketoconazole. *P < 0.05, **P < 0.01, ***P < 0.001, ##P < 0.01 and ###P < 0.001.

Supplementary Files

This is a list of supplementary files associated with this preprint. Click to download.

- SupplementaryFigure1.jpg
- SupplementaryTable1.doc
- SupplementaryTable2.docx
- SupplementaryTable3.docx
- SupplementaryTable4.docx
- SupplementaryTable5.docx
- SupplementaryTable6.docx